Research Article

Pulmonary Circulation

Cardiopulmonary remodeling in fattened beef cattle: a naturally occurring large animal model of obesity-associated pulmonary hypertension with left heart disease

Greta M. Krafsur[1,2,3], Joseph M. Neary[4], Franklyn Garry[5], Timothy Holt[5], Daniel H. Gould[2], Gary L. Mason[2], Milton G. Thomas[3], R. Mark Enns[3], Rubin M. Tuder[6], Michael P. Heaton[7], R. Dale Brown[1,*] and Kurt R. Stenmark[1,*]

[1]Department of Pediatrics, Critical Care Medicine and Cardiovascular Pulmonary Research Labs, University of Colorado Denver Anschutz School of Medicine, Aurora, CO, USA; [2]Department of Microbiology, Immunology and Pathology, Colorado State University, Fort Collins, CO, USA; [3]Department of Animal Sciences, Colorado State University, Fort Collins, CO, USA; [4]Department of Animal and Food Sciences, Texas Tech University, Lubbock, TX, USA; [5]Department of Clinical Sciences, Colorado State University College of Veterinary Medicine and Biomedical Sciences, Fort Collins, CO, USA; [6]Department of Pulmonary Sciences and Critical Care Medicine, Translational Lung Program, University of Colorado Denver Anschutz School of Medicine, Aurora, CO, USA; [7]Genetics, Breeding and Animal Health, United States Meat Animal Research Center, Clay Center, NE, USA

Abstract

The obesity epidemic in developed societies has led to increased cardiovascular diseases including pulmonary hypertension associated with left heart disease (PH-LHD), the largest and fastest-growing class of PH. Similar to obese humans, PH and heart failure (HF) are increasingly recognized in North American fattened beef cattle. We hypothesized that PH and HF in fattened beef cattle are novel, phenotypically distinct manifestations of bovine PH arising from left ventricular (LV) dysfunction similar to obesity-related PH-LHD in humans. We conducted a semi-quantitative histopathological assessment of cardiopulmonary tissues obtained from fattened beef cattle suffering end-stage HF compared to asymptomatic cattle of equivalent age undergoing the same fattening regimens. In HF animals we observed significant LV fibrosis, abundant cardiac adipose depots, coronary artery injury, and pulmonary venous remodeling recapitulating human obesity-related PH-LHD. Additionally, striking muscularization, medial hypertrophy, adventitial fibrosis, and vasa vasorum hyperplasia in the pulmonary arterial circulation were associated with sequela of pathologic right ventricular (RV) remodeling suggesting combined pulmonary venous and arterial hypertension. The association between obesity, pathologic cardiopulmonary remodeling, and HF in fattened beef cattle appears to recapitulate the complex pathophysiology of obesity-associated PH-LHD in humans. This novel, naturally occurring, and large animal model may provide mechanistic and translational insights into human disease.

Keywords

bronchopulmonary anastomoses, cardiac adiposity and fibrosis, obesity, pulmonary venous and arterial remodeling, small vessel disease

Date received: 17 July 2018; accepted: 3 August 2018

Pulmonary Circulation 2019; 9(1) 1–13
DOI: 10.1177/2045894018796804

Introduction

The obesity epidemic in Western societies has reached proportions where 37% of adults and 17% of youth residing in the United States are considered obese (body mass index [BMI] $\geq 30\,kg/m^2$)[1] and another 6.6% are categorized as morbidly obese (BMI $\geq 40\,kg/m^2$).[1] This syndrome has

*Equal contributors.

Corresponding author:
R. Dale Brown, Departments of Pediatrics and Medicine and Cardiovascular Pulmonary Research Laboratories, University of Colorado Anschutz Medical Campus, 12700 E. 19th Avenue, B131, Aurora, CO 80045, USA.
Email: Dale.Brow@UCDenver.edu

resulted in a growing burden of associated cardiovascular disease, including pulmonary hypertension with left heart disease (PH-LHD), defined as World Health Organization (WHO) Group 2 PH, the largest and fastest-growing category of PH worldwide.[2] Independent of the metabolic perturbations and vasculotoxic effects associated with obesity and the so-called metabolic syndrome, obesity-related fibrotic cardiac remodeling initiating diastolic dysfunction,[3] pulmonary venous hypertension,[4] atrial and ventricular arrhythmias,[5] and sudden cardiac death[6] are common adverse outcomes. Likewise, patients with LHD and PH fare worse than patients with LHD and no PH, including worsened survival and uncertain responses to vasodilator therapies.[7]

Despite the clinical importance of obesity-associated PH and LHD, knowledge of the mechanistic linkages is limited. This problem is exacerbated by the lack of translationally relevant animal models that recapitulate disease progression, hampering basic research and development of targeted therapies. The majority of studies have focused on rodent models of PH-LHD, many involving the use of surgical interventions, specialized inbred or genetically engineered strains.[8] Larger animal porcine models of PH-LHD (piglets or miniature swine) have utilized hemodynamic pressure overload of the left ventricle (LV) to generate PH and right ventricular (RV) dysfunction, independent of obesity[9] or obesity-induced LHD independent of PH.[10] While these approaches have yielded useful preclinical knowledge, the disparities between rodent and human cardiovascular physiology, the need for surgical intervention, and the complexities of heterogeneous patient populations limit translational utility of existing models and provide a impetus for development of naturally occurring, clinically relevant, large animal models.

Similar to increasing obesity in human populations, modern beef cattle production practices in the United States and Canada have achieved historic slaughter and carcass weights through combinations of genetic selection and intensive nutritional programs using megacalorie corn-based rations.[11] Strong similarities exist between body mass morphometrics of obese humans and fattened cattle, where cattle grading Choice or Prime (the most sought after grades for human consumption) have $> 30\%$ body fat[12] with enhanced accumulation of intramuscular adipose depots. These alterations in body morphometry have been accompanied by increased incidence of HF. HF deaths increased from 2 to 4 per 10,000 during 2000–2012 in 15 North American feedyards encompassing 1.56 million cattle.[13] Further, HF typically occurs late in the feeding cycle,[13,14] a phase characterized by maximal growth and accretion of adipose.[15] A longitudinal study of pulmonary arterial pressures (PAP) in Angus steers aged 6–18 months showed the greatest increase in PAPs occurred during the fattening phase,[13] suggesting susceptible individuals may be predisposed to increased risk of obesity-associated PH-LHD.

Based on these observations, we hypothesized that fattened beef cattle may provide a naturally occurring large animal model of PH-LHD. In this report, we present histopathologic findings from postmortem specimens of animals diagnosed with congestive heart failure (CHF), compared to asymptomatic controls of equivalent age and feeding practices, that recapitulate cardinal findings observed in human PH-LHD; namely, LV fibrosis, coronary vascular injury, and pulmonary venous remodeling. These findings were accompanied by evidence of attendant PA and RV remodeling, including striking muscularization, medial hypertrophy, adventitial expansion, and vasa vasorum hyperplasia in the PA circulation, together with RV fibrosis. Fibrotic transformation in the LV and RV myocardium was closely approximated with adipose depots and likewise adipose depots were characterized by mononuclear infiltrates, enhanced extracellular matrix, and frequently adipocytes encircled remodeled coronary arteries. The clinical diagnosis of CHF was confirmed microscopically by characteristic hepatic chronic passive congestion, centrilobular atrophy, and necrosis observed in end-stage disease.

Methods

On site postmortem examination of 15 commercial crossbred yearlings (11 steers, three heifers, one sex unknown not indicated at submission) occurred at low to moderate elevation feedyards (544-1420 m) in southeast Wyoming, northeast Colorado, and western Nebraska (See supplementary Table 1, online). Participating feedyards employed cattle feeding and marketing practices typical of the fed cattle industry with the capacity to simultaneously feed as many as 60,000 cattle. Economic and personnel constraints prohibited blood collection and invasive cardiopulmonary assessment of symptomatic animals, eliminating the need for institutional animal use and care approved protocols.

Cattle exhibiting intermandibular, sternal and ventral edema, shoulder abduction, jugular pulse or distended jugular veins, diarrhea, and loss of body condition were flagged as CHF, removed from the feeding program, and placed in hospital pens where they died or were euthanized using American Veterinary Medical Association approved techniques. Field necropsies were conducted by beef cattle veterinarians or feedyard staff highly experienced in recognizing gross pathology meeting the criteria for PH and CHF (hypertrophy/dilation of the right atrial and ventricular myocardium, dilated pulmonary trunk, hepatomegaly, ascites, mesenteric, mesocolonic and intestinal edema) and in distinguishing CHF from chronic pneumonia. Field necropsy practices limited tissue collection and preservation techniques to routine formalin-fixation without lung perfusion, precluding our ability to perform advanced stereomorphometic, immunohistochemical, ultrastructural, and molecular techniques.

Cardiopulmonary and hepatic tissues preserved in 10% buffered neutral formalin were assigned to an investigative veterinary pathologist specializing in production animal diseases (G. Krafsur). After complete formalin-fixation,

standard tissue sections were obtained from the heart (full thickness LV and RV papillary muscle with free wall), lungs (apex of the right cranioventral lung lobe, base of the right middle lung lobe, dorsal right diaphragmatic lung lobe), and liver. Trimmed tissues were embedded in paraffin, sectioned at 5 μm, and routinely stained with hematoxylin and eosin (H&E). Replicate sections from each heart and lung were additionally stained with Masson's trichrome (Masson's) for collagen and Verhoeff–Van Gieson (VVG) for collagen and elastic fibers. Pathologic cardiac and pulmonary remodeling, and hepatic chronic passive congestion (CPC), centrilobular necrosis (CLN), and bridging fibrosis, were semi-quantitatively evaluated as follows: 0 = no lesion; 1 = mild; 2 = moderate; and 3 = severe.

Understanding of bovine subgross pulmonary anatomy facilitated discrimination of pulmonary veins from pulmonary arteries. The bovine lung is conspicuously lobulated with generous fibrous connective tissue septa separating lobules, limiting available pathways to the bronchovascular tree and imposing a close anatomic relationship as the veins, arteries, and airways course the pulmonary parenchyma, with the bronchus situated between the vein and artery.[16] Pulmonary veins were distinguished from arterial vessels based on the presence of venous sphincters formed by abrupt disruption of the muscular media, imparting a beaded appearance in longitudinal sections (300–400 μm in diameter) and a crescentric appearance in cross-sections (150–300 μm in diameter).[17] Veins in the range of 20–150 μm in diameter possessed a thick muscular media and were discriminated from arteries based upon intermittent to absent internal elastic membranes visualized with VVG staining.[18] Ramifications of the bronchial artery encircled airway walls and formed intermittent branches to the pulmonary artery in the form of the vasa vasorum.[19]

Evaluation of the myocardium was based on criteria used in the evaluation of human endomyocardial biopsy specimens, assessing perivascular, interstitial, and replacement fibrosis.[20] Cardiac adiposity, inflammatory infiltrate, type, and distribution were assessed on H&E-stained sections of both the LV and RV myocardium using semi-quantitative analysis. Myocardial specimens were evaluated for the patency of epicardial coronary arteries and pathologic alterations in the intramural coronary arteries. Detailed description of the criteria and grading scheme for evaluation of cardiopulmonary tissue is provided (See supplementary Tables 2 and 3, online).

Cardiopulmonary tissues from asymptomatic yearling beef cattle subjected to analogous feeding and management practices to symptomatic cattle were obtained for comparison from a northeastern Colorado processing plant (elevation 1420 m) that contracts fattened cattle from small and large feeding facilities across the High Plains states, processing nearly 5500 beef cattle per day. Case control cattle were therefore representative of the cattle supplying the nation's beef inventory and comparable to CHF animals. Carcass weights, provided by the processor, were used to estimate the live weights of case control cattle[21] (See supplementary Table 1, online).

Cardiopulmonary specimens from case control cattle were prepared and evaluated analogous to those obtained from symptomatic cattle (See supplementary Tables 2 and 3, online). Hepatic tissues from case control cattle were not available because of their retail value to the processing plant, although hepatic tissue from an age- and weight-matched fattened steer was obtained for the purpose of illustration.

Statistical analysis

Histopathologic data are quantitated as raw scores with the mean ± SD. Comparisons were made between the two groups using unpaired Student's t tests. Data marked with asterisks are significantly different from the control group as follows: $P = \text{ns}$ ($P > 0.05$); $^{*}P < 0.05$; $^{**}P < 0.01$; $^{***}P < 0.001$.

Results

Characteristics of feedyard end-stage CHF and healthy beef cattle completing the feeding cycle

Cattle succumbing to PH and CHF were sourced from low to moderate elevation breeding programs for placement in feedyards scattered across the High Plains. Symptomatic cattle were within 30 days of harvest and thus had undergone prolonged fattening on a high-energy, corn-based diet to elicit rapid growth and deposition of intramuscular adipose. The majority of affected cattle were steers (11/14). Cattle exhibiting characteristic intermandibular, sternal and ventral edema, jugular vein pulse, and distention (Fig. 1) were flagged by feedyard staff as CHF, pulled from the feeding program, and placed in hospital pens for surveillance and resolution of generalized anasarca before harvest at processing facilities specializing in the receipt of animals not intended for human consumption. Twelve of the 15 animals died before sale to the alternative processing plant and the remaining three were euthanized. The origin, history, and gender of healthy case control cattle completing the feeding cycle were not accessible; however, clinical illness could be ruled out in case control animals because they entered a processing plant supplying the global food chain and carcasses passed USDA meat inspection. Healthy case control cattle live market weights were estimated from the hot carcass weights provided by the processor (Avg. = 676 kg, SD = ± 64 kg; See supplementary Table 1, online).

Cardiac fibrosis, adiposity, inflammation, and coronary artery pathology

Cardiac fibrosis. Masson's staining of histologic sections of LV myocardium revealed perivascular, interstitial, and replacement fibrosis in symptomatic cattle (Fig. 2).

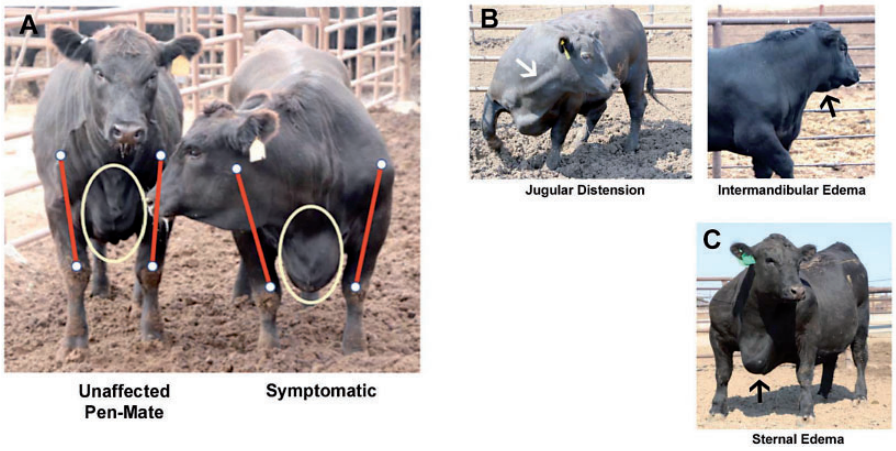

Fig. 1. Clinical signs of PH and CHF. (a) Symptomatic animal alongside healthy pen-mate. White oval delineates accumulation of fluid in the sternal subcutaneous tissues (symptomatic) compared to no accumulation of fluid in the sternal subcutaneous tissues of the healthy pen-mate. Red lines with closed white circles highlight shoulder abduction in the symptomatic animal compared to the healthy pen-mate due to accumulation of edema fluid in the sternum. (b) Arrow points to striking jugular vein distention (left) and intermandibular edema (right). (c) Arrow points to noteworthy accumulation of fluid in the sternal subcutaneous tissues accompanied by marked shoulder abduction.

Perivascular (Fig. 2d, 2m) and interstitial fibrosis (Fig. 2e, 2n) were evident in all histologic sections of LV myocardium from symptomatic cattle. Interstitial fibrosis ranged from mild and patchy to severe and diffuse, often with tendrils of collagenous matrix dissecting between, enveloping, and isolating individual and groups of cardiomyocytes. Variable replacement fibrosis, ranging from mild to severe postnecrotic scarring, was visualized (Fig. 2f, 2o). LV myocytes were frequently haphazardly arranged in a herringbone or pinwheel configuration around foci of interstitial collagen. Myocyte disarray was genuine because care was taken to avoid taking samples where the anterior and posterior walls of the ventricle interdigitate with the septum, a location known to display inherent myocyte disarray. The LV myocardium of case control cattle exhibited significantly less perivascular (Fig. 2a) and interstitial fibrosis (Fig. 2b), although two apparently healthy case control animals (Case Controls 16, 20) completed the production cycle despite exhibiting noteworthy interstitial fibrosis and myocyte disarray, and mild perivascular and replacement fibrosis (Fig. 2c), suggesting subclinical heart disease in these two animals.

Cardiac RV perivascular (Fig. 2j, 2p), interstitial (Fig. 2k, 2q), and replacement fibrosis (Fig. 2l, 2r) were expectedly greater in symptomatic cattle compared to control cattle (Fig. 2g–i). Replacement fibrosis was detected in the RV myocardium of one of the 20 case control animals (Fig. 2i) and was not present in those with noteworthy LV fibrosis as mentioned (Case Controls 16, 20).

Adiposity and inflammation. Epicardial adipose tissue (EAT) contiguous with the LV and RV myocardium and following the adventitia of the major coronary artery branches formed conspicuous isles and linear bands of adipocytes in the subepicardial LV and RV myocardium, incorporating loose fibrocollagenous matrix (Fig. 3, Panel 1a–d) The perivascular adventitial matrix in the LV and RV myocardium was bounded by conspicuous fatty infiltrate formed by white adipocytes containing a single large lipid droplet compressing and peripheralizing the nucleus. Adipocytes infiltrating and tracing the cardiac interstitium frequently permeated the entire thickness of the LV and RV myocardium, encircling Purkinje fibers and nerve bundles. Moreover, both LV and RV EAT exhibited accompanying fibrotic remodeling with tendrils of collagen emanating from the EAT, infiltrating the subepicardium and thickening the interstitium (Fig. 3, Panel 1e, 1f), and encircling Purkinje fibers and nerve bundles in the subendocardium (Fig. 3, Panel 1g, 1h). Subepicardial, perivascular, and interstitial LV and RV adipose depots were populated by moderate to marked lymphomononuclear infiltrate (Fig. 3, Panel 1a, 1b) and loose fibrocollagenous matrix (Fig. 3, Panel 1c, 1d). Numerous mononuclear cells with large undulating *caterpillar-like* nuclear chromatin, so-called cardiac histiocytes or Anchikov cells tended to colocalize in the perivascular adipose depots (Fig. 3, Panel 1c, 1d).The microscopic quantitation of perivascular adipose and mononuclear infiltrates is summarized in Fig. 3 Panel 2a–d. Field sampling and preservation techniques prohibited assessment of intramyocytic lipid accumulation in affected cattle.

Coronary vascular remodeling. Considerable periadventitial and perineural fibrosis and infiltration of the subepicardium by fibrocollagenous matrix extending from the expanded adventitia delineating the epicardial coronary arteries was observed in affected animals (Fig. 3). Major branches of the coronary arteries and small intramural coronary arteries (50–100 μm) in the LV myocardium were frequently narrowed due to neointimal hyperplasia, fibromuscularization, and dramatic circumferential adventitial fibrosis obscuring

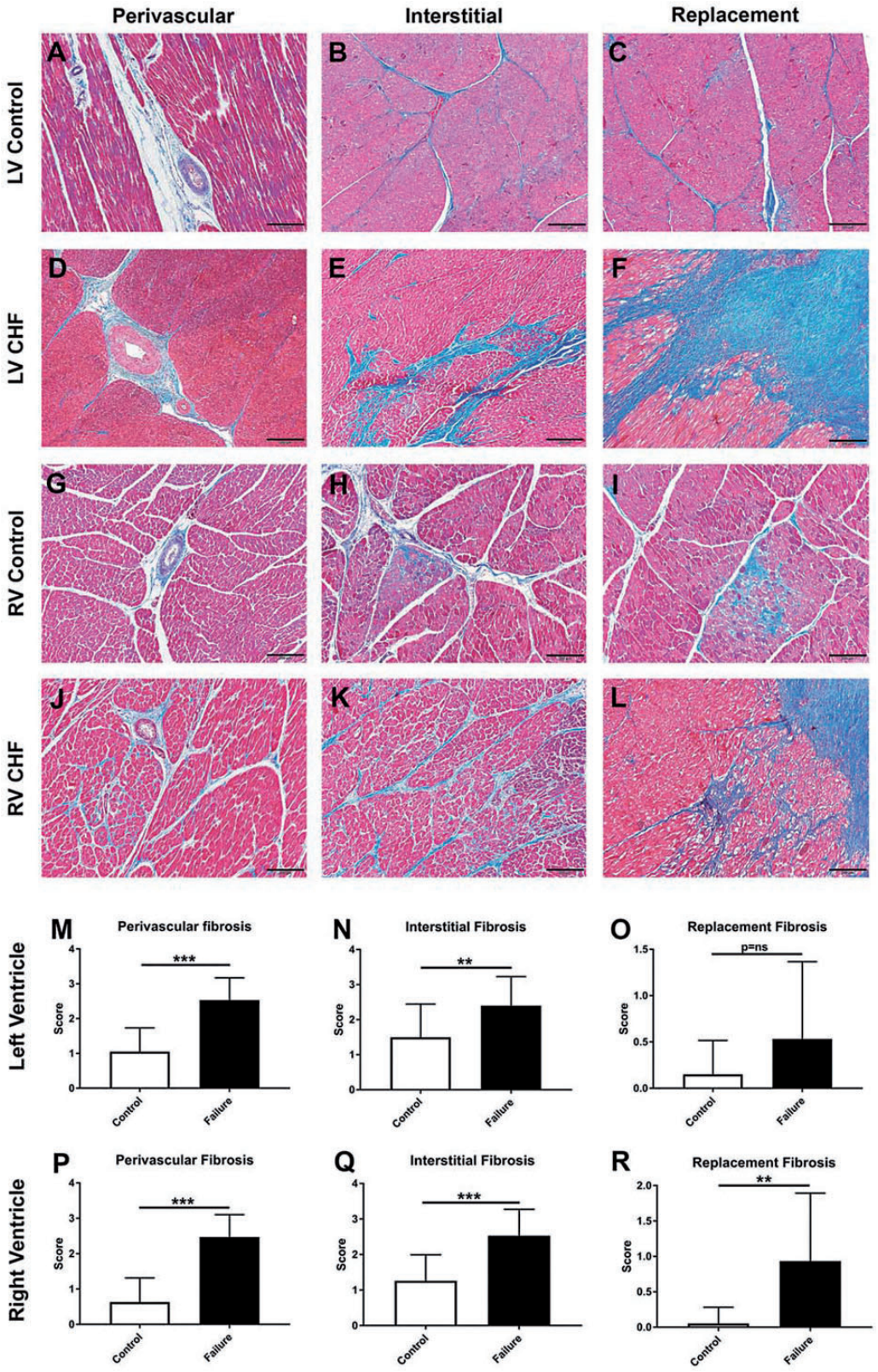

Fig. 2. Cardiac fibrosis. (a–l) Representative images of the LV and RV myocardium from feedyard case control (a–c, g–i) and cattle with congestive heart failure (d–f, j–l). Feedyard cattle with CHF have LV perivascular (d), interstitial (e), and replacement (f) fibrosis compared to the control (a–c). RV perivascular (j), interstitial (k), and replacement (l) fibrosis of symptomatic cattle compared to the case control (g–i). Semi-quantitative microscopic assessment for cardiac fibrosis: LV perivascular fibrosis (m), LV interstitial fibrosis (n), LV replacement fibrosis (o), RV perivascular fibrosis (p), RV interstitial fibrosis (q), RV replacement fibrosis (r). (a–l) Masson's Trichrome. Scale bars: 200 μm. (m–r) $P = \text{ns}$ (> 0.05), $^{*}P < 0.05$, $^{**}P < 0.01$, $^{***}P < 0.001$.

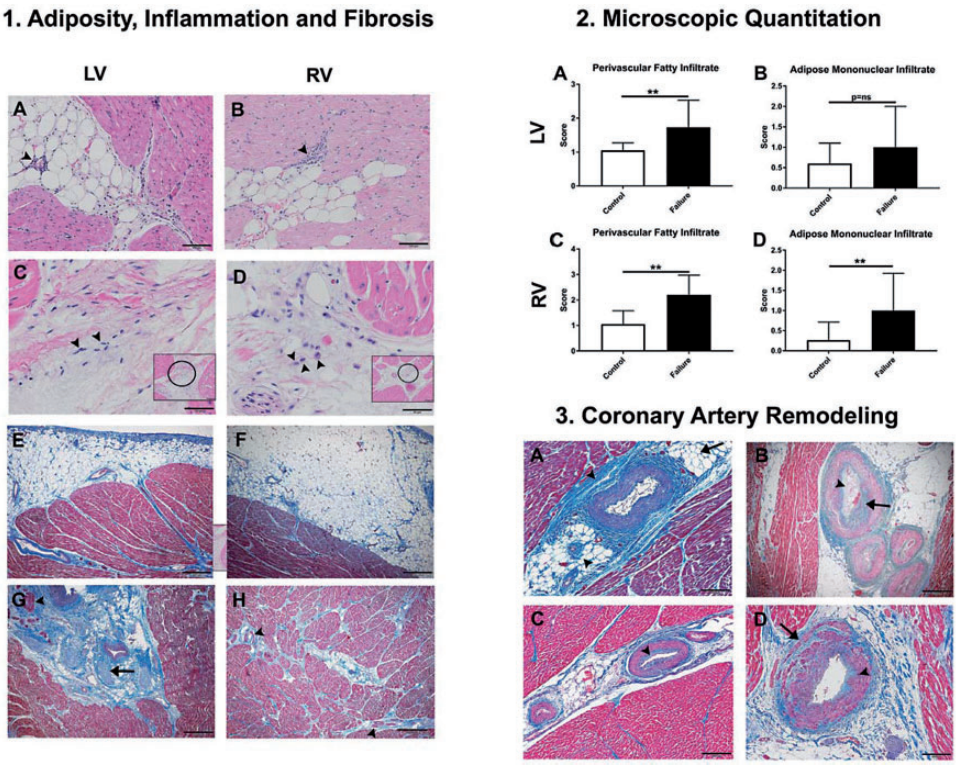

Fig. 3. Cardiac adiposity, mononuclear inflammation, and fibrosis with coronary artery disease. Panel 1: Adiposity, inflammation, and fibrosis. (a–h) Representative images of LV and RV adiposity, mononuclear inflammation, and fibrosis in CHF. (a) LV fatty infiltrate with mononuclear inflammation (arrowhead). (b) RV fatty infiltrate with mononuclear inflammation (arrowhead). (c) LV with enhanced extracellular matrix and cardiac histiocytes (inset, 200×) and 400 × magnification of numerous cardiac histiocytes (arrowheads). (d) RV with enhanced extracellular matrix and cardiac histiocytes (inset, 100×) and 400 × magnification of numerous cardiac histiocytes (arrowheads). LV (e) and RV (f) EAT with fibrotic transformation and tendrils of collagen permeating the subepicardium. (g) Abundant PVAT and fibrosis encircling Purkinje fibers (arrowhead) and nerve bundles (arrow). (h) RV with fibrotic transformation of PVAT, interstitial compartments, and peri-Purkinje fiber fibrosis (arrowheads). Panel 2: Microscopic quantitation. LV perivascular fatty infiltrate (a), LV adipose mononuclear infiltrate (b), RV perivascular fatty infiltrate (c), RV adipose mononuclear infiltrate (d). Panel 3: Coronary artery remodeling. (a–d) Peri-coronary adipose depots have increased extracellular matrix and periadventitial fibrosis with collagen invasion and disruption of major branches of the coronary arteries, fibromuscular hypertrophy, and neointimal lesions. (a) Arrow indicates LV peri-coronary adipose depot with increased extracellular matrix, arrowheads point to branches of coronary artery supplying the LV myocardium delineated by conspicuous periadventitial fibrosis. (b) Branches of the coronary artery supplying the LV myocardium with collagenous expansion of the muscular coat (arrow) and neointimal lesion (arrowhead). (c) LV intramural coronary artery with enhanced collagen (arrowhead). (d) Branch of the coronary artery supplying the RV myocardium depicting collagen invasion of the muscular coat (arrow) and subintimal collagen deposition (arrowhead). Panel 1: (a–d) H&E. Scale bars: 50 μm (c, d); 100 μm (a–c inset); 200 μm (d inset). (e–h) Masson's Trichrome. Scale bars: 500 μm. Panel 2: (a–d) P = ns (> 0.05), *$P < 0.05$, **$P < 0.01$, ***$P < 0.001$. Panel 3: (a–d) Masson's Trichrome. Scale bars: 200 μm.

abundant perivascular adipose depots with fibrous tendrils infiltrating adjacent cardiac interstitium (10/15 LV; Fig. 3 Panel 3a–c). It is important to note that six of the healthy case controls, including the two animals with noteworthy LV fibrosis (Case Controls 16, 20) also had evidence of mild remodeling to the major branches of the coronary arteries and small intramural coronary arteries supplying the LV myocardium. Coronary artery pathology was observed occasionally in the major branches and small intramural coronary arteries supplying the RV myocardium (5 out of 15 symptomatic animals, Fig. 3, Panel 3d), but was uniformly present in the corresponding LV. None or minimal injury to the coronary arteries supplying the RV myocardium was noted in the case control animals.

Epicardial coronary arteries supplying the LV and RV EAT and myocardium were patent in diseased cattle, exhibiting infrequent and minimal neointimal hyperplasia.

Pulmonary veno-arterial remodeling. Significant luminal narrowing and occlusion of intrapulmonary veins, defined as serial focal constrictions arising from hypertrophied venous sphincters, were observed in symptomatic cattle compared to case control cattle (Fig. 4a–c, 4e–p). Intrapulmonary veins of symptomatic cattle also featured expanded adventitial matrix due to added collagen (Fig. 4b, 4d, 4f–h, 4j–l, 4n–p). Microscopic alterations in the PA circulation of cattle with end-stage CHF included: neomuscularization of normally nonmuscularized arterioles (< 50 μm); medial

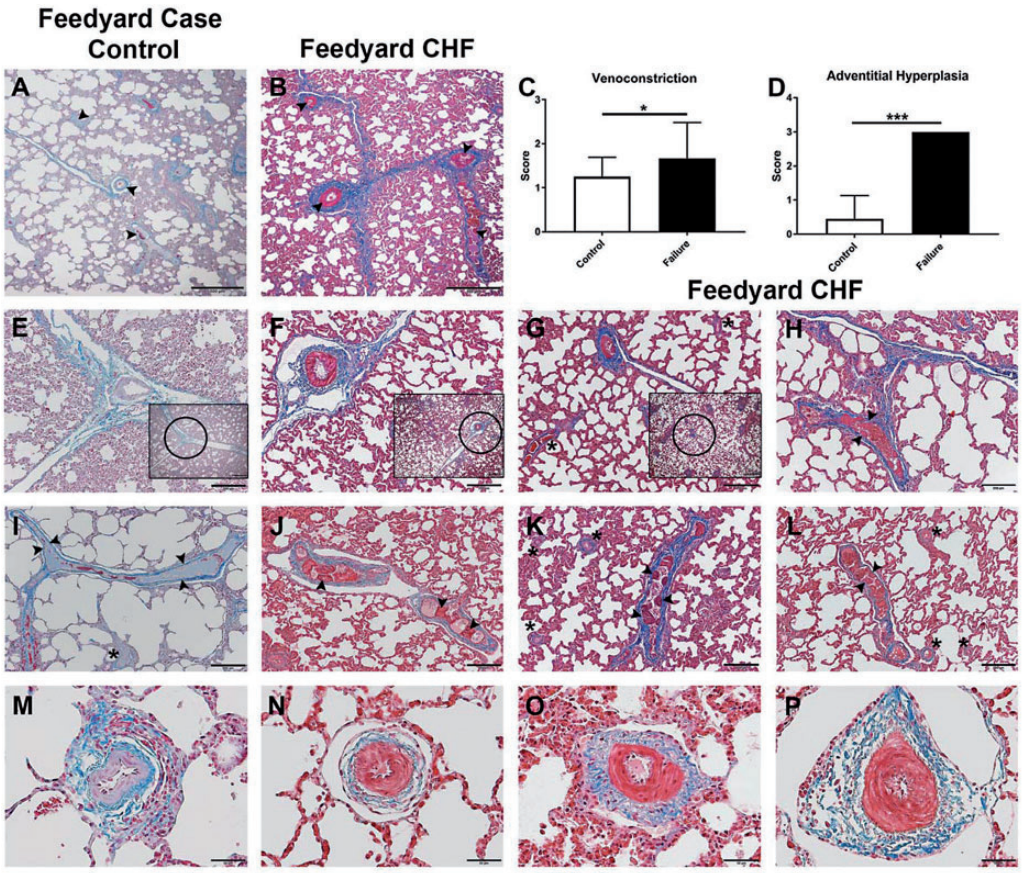

Fig. 4. Pulmonary venous remodeling. (a, b, e–p) Representative images of the pulmonary veins from case control cattle (a, e, i, m) and cattle with CHF (b, f–h, j–l, n–p). Septal veins in symptomatic animal (b) are narrowed due to venoconstriction (arrowheads) and circumscribed by conspicuous adventitial fibrosis compared to control animal (a). Arrowheads (a) point to veins with patent lumina and inconspicuous venous sphincters. (f–h) Septal veins exhibit serial narrowing and occlusion due to hypertrophied venous sphincters compared to control animal (e) with relaxed venous sphincters. (g) Hypertrophied venous sphincters in pre-septal veins (asterisks). (h) Longitudinal section of congested septal vein with hypertrophied venous sphincters (arrowheads). The symptomatic animals (f–h) have prominent perivenular adventitial fibrosis compared to the control (e). (j–l) Longitudinal sections of septal veins with hypertrophied venous sphincters (arrowheads) and perivenular adventitial fibrosis compared to the control (i). Asterisks (k, l) indicate pre-septal veins with hypertrophied venous sphincters. (n–p) Impressively hypertrophied venous sphincters and perivenular adventitial expansion in septal veins compared to the control (m). Semi-quantitative microscopic assessment of pulmonary venous remodeling: pulmonary venoconstriction (c), perivenular adventitial hyperplasia (d). (a, b, e–p) Masson's Trichrome. Scale bars: 500 μm (a, b, e–g insets); 200 μm (e–l); 50 μm (m–p). (c, d) $P = \text{ns}$ (> 0.05), $^{*}P < 0.05$, $^{**}P < 0.01$, $^{***}P < 0.001$.

hypertrophy of proximal muscular pulmonary arteries; and adventitial fibrosis (Fig. 5b–i, 5k–n). Conspicuous tertiary lymphoid organs, largely converging on the airways forming bronchus-associated lymphoid tissue, were consistently enhanced in symptomatic cattle compared to case controls (Fig. 5o–q).

Remodeling of the pulmonary microcirculation. In addition to remodeling of existing vessels, striking vasa vasorum neovascularization in the adventitial and medial compartments of pulmonary arteries was a regular feature in symptomatic cattle (Fig. 6a–h). Further, vessel ingrowth extended along the length of the vascular tree and was especially impressive in the adventitial matrix of small vessels (50 μm, Fig. 6c, 6h). The peribronchial microcirculation was conspicuously dilated and congested (Fig. 7a, 7a', 7b, 7b', 7b'') with focal peribronchial edema (Fig. 7a, 7b') and hemorrhage (Fig. 7c, 7c'). Patchy to diffuse interstitial capillary remodeling was a consistent finding in symptomatic cattle and included alveolar septal thickening due to severe focal capillary congestion and multiplication resembling pulmonary capillary hemangiomatosis (Fig. 7d, 7e), with focal intra-alveolar hemorrhage, intra-alveolar macrophages, erythrophages and siderophages (Fig. 7d, 7e), and leukocytic infiltrates largely comprising lymphomonuclear cells (Fig. 7f, 7g).

Hepatic chronic passive congestion, centrilobular necrosis, and fatty degeneration. As expected for endstage CHF, characteristic features of chronic passive congestion (CPC) of the liver

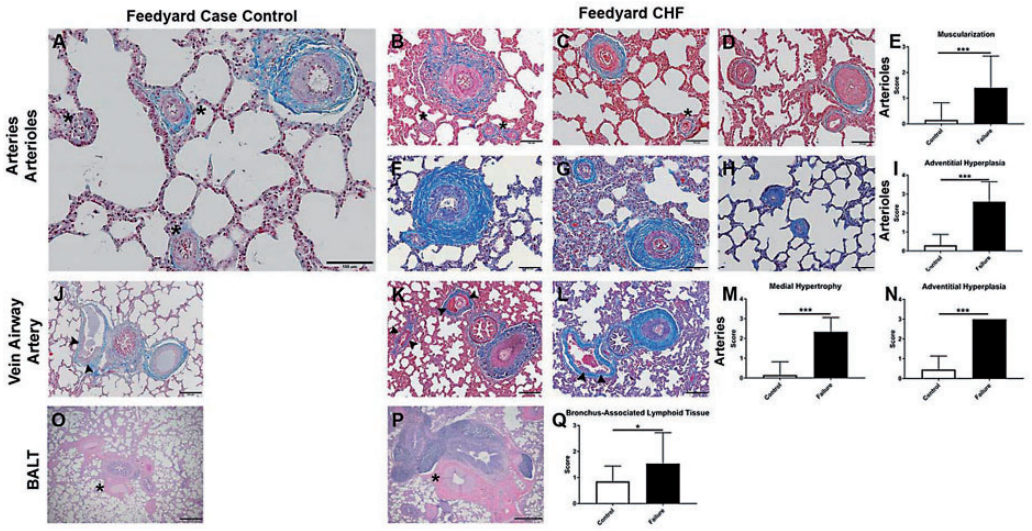

Fig. 5. Pulmonary arterial remodeling. (a–d, f–h, j–l, o–p) Representative images of the pulmonary arterial circulation and bronchus-associated lymphoid tissue of case control cattle (a, j, o) and cattle with CHF (b–d, e–h, k, l, p). Striking muscularization, medial hypertrophy, and adventitial fibrosis in the pulmonary arteries and arterioles of CHF cattle (b–d, e–h) compared to control (a). (k–l) Impressive adventitial fibrosis delineating veins and arteries neighboring airways, arterial medial hypertrophy, and mildly hypertrophied venous sphincters (arrowheads) compared to the control (j). (p) Marked BALT hyperplasia, dramatic adventitial fibrosis, and medial hypertrophy of pulmonary artery (asterisk) compared to control (o). Semi-quantitative microscopic assessment of pulmonary arterial remodeling: pulmonary arteriole muscularization (e), pulmonary arteriole adventitial hyperplasia (i), pulmonary artery medial hypertrophy (m), pulmonary artery adventitial hyperplasia (n), bronchus-associated lymphoid tissue (q). (a–d, f–h, j–l) Masson's Trichrome. Scale bars: 200 μm (j–l); 100 μm (a–d, f, h). (o, p) H&E. Scale bars: 500 μm. (e, i, mn, n, q) $P = \text{ns}$ (> 0.05), $^{*}P < 0.05$, $^{**}P < 0.01$, $^{***}P < 0.001$.

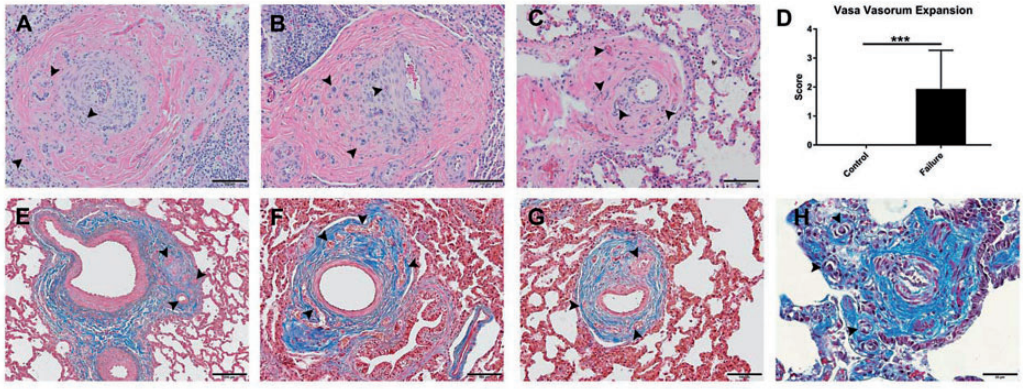

Fig. 6. Vasa vasorum neovascularization. Representative images of striking vasa vasorum neovascularization in CHF cattle (a–c, e–h). Arrowheads point to examples of vessel ingrowth. (d) Semi-quantitative microscopic assessment of expanded vasa vasorum. (a–c) H&E. Scale bars: 100 μm. (d) $P = \text{ns}$ (> 0.05), $^{*}P < 0.05$, $^{**}P < 0.01$, $^{***}P < 0.001$. (e–h) Masson's Trichrome. Scale bars: 200 μm (e); 100 μm (f, g); 50 μm (h).

with fibrous plaques in Glisson's capsule and centrilobular necrosis (CLN) were observed in symptomatic animals (Fig. 8). In CPC and CLN, portal hepatocytes were generally well-preserved while hepatic cords surrounding central veins were severely atrophied, separated by dilated sinusoids with increased prominence of the space of Disse and pale-staining central hepatocytes due to coagulative necrosis. The most extreme cases of congestion and hepatocellular injury exhibited diffuse bridging centrilobular atrophy and collapse of the reticulin network, centrilobular fibrosis bridging terminal hepatic venules with fibrous septa dissecting between lobules and severe midzonal to periportal macrovesicular hepatocellular steatosis (Fig. 8b, 8d). Swollen hepatocytes enlarged by a single large lipid vacuole displacing and peripheralizing the nucleus characterized hepatic steatosis (Fig. 8b, 8d). Hepatic function could not be assessed due to the inavailability of blood for serum chemistry analysis.

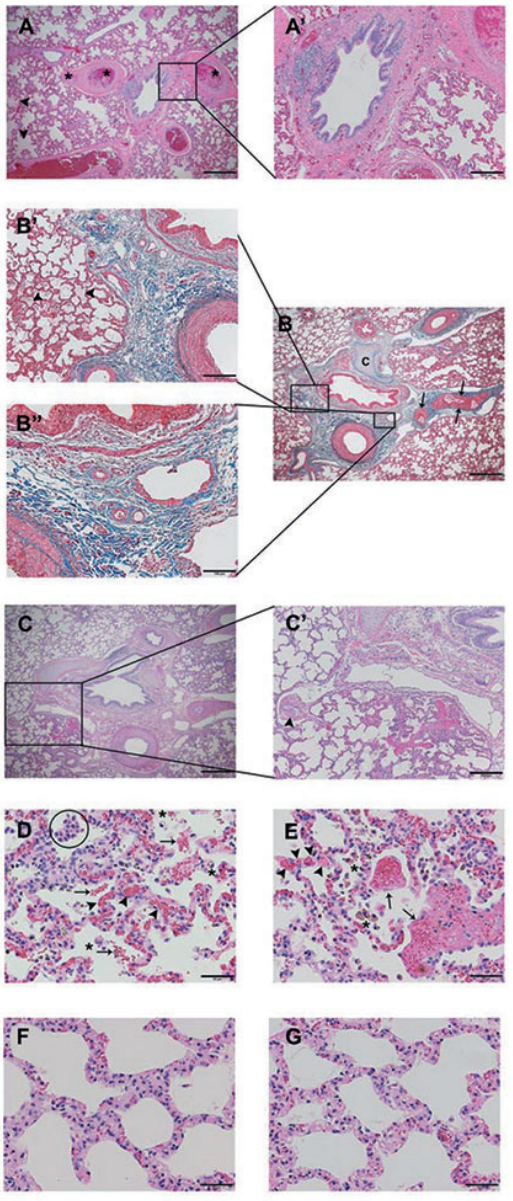

Fig. 7. Peribronchial and Interstitial Remodeling. Representative images of congestion and dilation of the bronchial microcirculation (a, a', b, b', b") with focal edema (arrowheads, a, b'), multifocal thrombi (a, asterisks), hypertrophied pulmonary venous sphincters (b, arrows), and cartilage (c). (c, c') Peribronchial hemorrhage and hypertrophied pulmonary venous sphincter (c', arrowhead). (d, e) Capillary congestion and multiplication (arrowheads) with intra-alveolar hemorrhage (arrows), intra-alveolar erythrophages, siderophages (asterisks), and macrophages (circle). (f, g) Interstitium thickened by lymphomononuclear infiltrate. (a, a', c, c', d–g) H&E. Scale bars: 500 μm (a, c); 200 μm (a', c'); 50 μm (d–g). (b, b', b") Masson's Trichrome. Scale bars: 500 μm (b); 200 μm (b'); 100 μm (b").

Discussion

We show here that cattle suffering from CHF during periods of intense fattening exhibit histopathologic features of cardiac and pulmonary remodeling consistent with obesity-associated PH-LHD. Herein, we provide the first formal description of LV pathologic alterations with combined pulmonary venous and arterial remodeling, RV and coronary artery pathology, and striking cardiac adiposity in affected animals. Our findings suggest the etiology of PH-LHD in fattened beef cattle is a complex, multistep process ultimately generating biventricular dysfunction and vascular remodeling involving all segments of the pulmonary vascular bed. We propose that intensive fattening leads to dysregulation of metabolic, vascular, and inflammatory pathways resulting in LV fibrosis and intracardiac adipose deposition leading to LV stiffening and diastolic dysfunction. The elevated LV diastolic filling pressure in turn causes hypertrophic remodeling and adventitial expansion of the pulmonary venous circulation as well as pulmonary venous hypertension. This scenario is supported by our data showing LV fibrotic remodeling, striking pulmonary venous muscularization, venoclusion, and perivenular adventitial hyperplasia.

The severity of lesions in the precapillary circulation are suggestive of greater than anticipated ("out of proportion") elevations in PAP for a given increase in pulmonary venous pressure, consistent with combined post- and pre-capillary PH in susceptible individuals.[22,23] Precapillary pulmonary arteriolar remodeling in these individuals would generate elevated pulmonary vascular resistance (PVR) and augmented transpulmonary and diastolic pulmonary pressure gradients.[24] The sustained elevation of RV afterload, together with perivascular and interstitial adipose deposition within the RV similar to LV, would then drive predicted outcomes of pathologic RV remodeling, dysfunction, and failure. Elevated central venous pressure arising from RV dysfunction initiates congestive hepatopathy with centrilobular atrophy, necrosis, and cardiac cirrhosis, as we observe in the end-stage CHF animals.

Our observations of pulmonary venous and bronchial remodeling, impressive vasa vasorum hyperplasia, and capillary hemangiomatosis-like lesions suggest for the first time, a naturally occurring animal model exhibiting the constellation of pulmonary microvasculopathy, termed small-vessel disease, that influences illness severity and clinical outcomes across multiple classes of PH, particularly CTEPH,[21,25] IPAH,[26] COPD-PH,[26] and PH-LHD with preserved or reduced ejection fraction.[27,28] Emerging anatomic evidence suggests post-capillary bronchopulmonary anastomoses are generated in the context of elevated PVR, shunting blood away from the high-pressure bronchial (systemic) circulation to the low-pressure pulmonary venous system.[21,29] The resulting hemodynamic stresses initiate venous reactivity and pathologic venous and microvascular remodeling with consequential capillary congestion and proliferation.[21,29] Moreover, bronchopulmonary anastomoses in the bovine lung[19] might counteract perturbations in pulmonary blood flow associated with obstructive lesions in the arterial circulation and faciliate vasa vasorum hyperplasia and plexiform lesion development.[30]

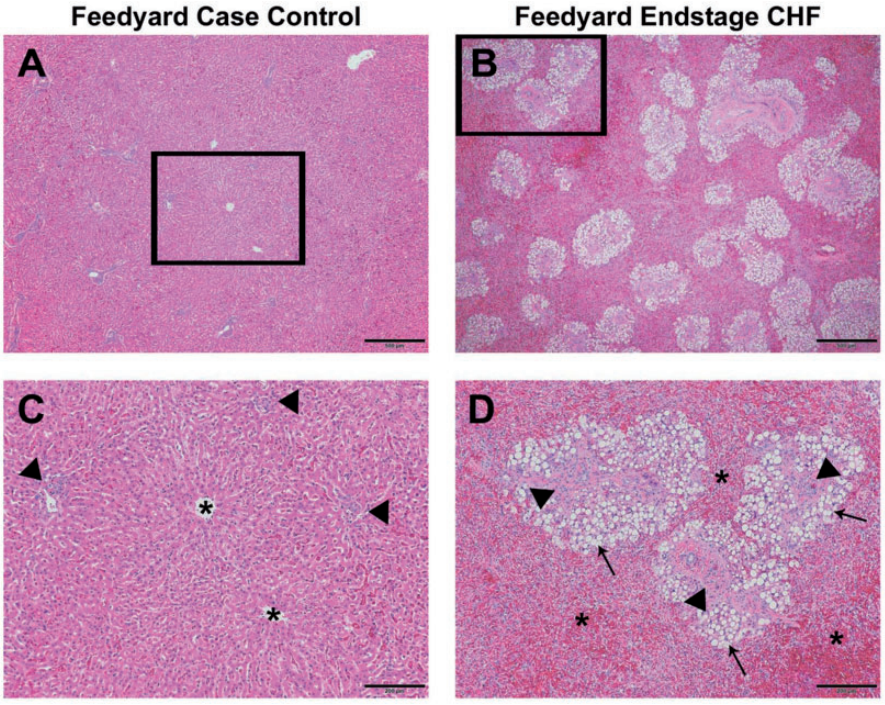

Fig. 8. Hepatic Lesions. (a–d) Representative images of hepatic parenchyma from age-matched fattened steer (a, c) and animal with CHF (b, d). Boxed areas (a, b) are shown at higher magnification in the panels below them (c, d). (b, d) Severe bridging centrilobular atrophy (asterisks), midzonal to periportal hepatocellular steatosis (arrows) and massive periportal adventitial fibrosis (arrrowheads) compared to intact hepatocellular cords surrounding central veins (asterisks) and inconspicuous portal tracts (arrowheads) in age-matched fattened steer (a, c). H&E. Scale bars: 500 μm (a, b); 200 μm (c, d).

Striking evidence of perivascular-coronary and interstitial adipose accumulation in both RV and LV of PH-LHD animals was observed. We speculate that intracardiac adipose depots derived from EAT may be an important mechanism of pathological myocardial remodeling in obesity. Similar to many obese humans, fattened beef cattle tend to have profuse visceral fat depots, particularly EAT.[31] EAT is composed of mature adipocytes and adipocyte precursors, a stromovascular fraction populated by macrophages, fibroblasts, and endothelial cells, and interconnecting nerves and ganglia.[32,33] Structurally and functionally, EAT is intimately associated with the myocardium because of the absence of fascial boundaries and a shared microcirculation.[32,33] Mature adipocytes can permeate the underlying myocardium and course along the adventitia of the major branches of the coronary arteries forming depots of perivascular adipose tissue.[32,33] EAT is a metabolically active endocrine organ involved in lipid and energy homeostasis and secretion of bioactive molecules that can either protect or adversely affect the myocardium and coronary arteries.[34] EAT has a far greater capacity for uptake and release of free fatty acids (FFAs) than other visceral adipose depots and in health EAT protects the heart by acting as a buffer for excess arterial FFAs, storing them and releasing them to the myocardium during times of high energy demand.[35] Healthy EAT secretes protective adipocytokines influencing local vascular tone by increasing nitric oxide bioavailability and promoting an anti-inflammatory, anti-atherogenic microenvironment.[36]

Obesity-induced pathologic expansion of EAT, however, is associated with an unfavorable phenotypic transformation resulting in elaboration of pro-inflammatory, pro-atherogenic molecules, and striking lymphomononuclear inflammation.[37–40] Accordingly, paracrine dialog between adipocytes and pro-inflammatory macrophages perpetuates a relentless cycle of chronic inflammation in the adipose of obese patients.[37,41] Furthermore, dysfunctional adipose tissue is phenotypically pro-fibrotic owing to secretion of adipo-fibrokines.[42] Cross-talk between EAT and the underlying myocardium facilitates cardiac fibrosis[43] and may lead to increased LV mass,[44] deteriorating LV diastolic function,[45] atrial fibrillation,[5,42] and pulmonary venous hypertension.[4] EAT is emerging as a significant cardiac risk factor and cardiotherapeutic target whose accretion is more predictive of risk for cardiovascular disease than traditional anthropometric measures used to quantify adiposity such as BMI and waist circumference.[46] Considering the virtual absence of EAT in murid rodents,[35] fattened beef cattle provide a feasible alternative to elucidate the mechanistic role of EAT in metabolic-related cardiovascular disease.

The cattle used in this study were from low to moderate elevation breeding programs. Regardless of feedlot location,

cattle were similarly managed and fed to comparable endpoints using prototypical animal health and production practices developed by feedlot veterinarians and nutritionists. Heifers entering feeding programs are routinely administered melengesterol acetate in the feeding ration or ovariectomized to suppress estrus.[47] Limited sample size precludes our ability to draw conclusions regarding sex influence and the role of estrogen (E_2) in the development of bovine PH. Regardless of gender differences, symptomatic and healthy cattle in this study were all in the high-concentrate phase of the fattening diet, and were fed at least 80% corn and corn-ethanol byproducts mixed with roughage (alfalfa hay, alfalfa, or corn silage) and supplemental fats. Feedstuff, used to fatten beef cattle, recapitulate features of a Western diet, where lower caloric density hay and forage have been replaced by cheaper, abundant corn and corn ethanol byproducts high in digestible and metabolisable energy, starches, sugars, and oils.[48] Moreover, the triacylglycrerols in corn-based feedstuffs largely comprise C_{18} polyunsaturated fatty acids (18:2 and 18:3, linoleic, and linolenic acid) that are progressively hydrolyzed to a large extent by rumen bacteria to stearic acid and deposited as saturated fats.[48] The increases in cardiopulmonary disease associated with intensive fattening in beef cattle parallel observations in swine[49,50] and poultry,[51] food animals that are increasingly fed corn-based diets. Of note, pathologic structural and functional alterations in the left heart of fast-growing broiler chickens have been shown to play a significant role in the natural history of ascites syndrome, preceding and influencing the hemodynamic changes leading to PH and RHF.[52,53]

Death loss attributed to PH and CHF in three Northern Colorado feedyards accounted for up to almost 10% of mortalities in 2014. Of this group, HF mortalities as a percent of total mortalities by days on feed were greatest in the final days of the feeding period and accounted for nearly 12% of mortalities in cattle more than 140 days on feed (personal communication to G.M. Krafsur, D.V.M.-Ph.D. Trainee, Veterinary Pathologist and Co-Investigator). Coincidentally, the onset of PH and CHF in low to moderate elevation beef cattle parallels the shift from primarily grass to corn-fed beef. Interestingly, whereas the average live market weight for feeder cattle has increased by 48%—from 400 kg in 1944 to ~600 kg in 2016[11]—a concomitant increase in cardiac mass has not been observed. Taken together, these observations emphasize that modern domestic food animals may provide important translational insights into mechanisms of obesity-induced cardiovascular disease in the humans who consume them.

Some limitations of the present studies point to important directions for further research. First, it is essential to confirm and complement these histopathologic findings with hemodynamic and echocardiographic assessment of cardiac function in vivo. Obesity is associated with both systolic and diastolic cardiac dysfunction resulting, respectively, in HF with reduced or preserved ejection fraction.[54] The observations of cardiac fibrosis and pulmonary venous remodeling clearly argue for diastolic dysfunction; however, substantial perivascular and interstitial adipose deposition may impair cardiac perfusion and cause systolic dysfunction as well. Longitudinal study of animals throughout the fattening cycle can provide important insights into the detection, progression, and prevention of obesity-related PH-LHD. In addition, it will be important to compare the evidence of cardiopulmonary remodeling in these animals subjected to intensive fattening, with grass-fed animals developed to equivalent ages over longer time intervals with non-corn diets.

In conclusion, we present here histopathological evidence for a novel and naturally occurring, large animal model of obesity-associated PH-LHD that features cardiac fibrosis and adipose deposition, and pulmonary venous and arterial remodeling, similar to human disease. This animal model should provide a platform for developing novel approaches to detection, prevention, and therapy of this major condition affecting the global burden of human cardiovascular disease.

Acknowledgments

The authors thank Iskra Majewski, Maddi Funk (CSU CATS Lab), Todd Bass, and Wendy Cottrell (CSU Histotechnology Lab) for their technical expertise in the preparation of this manuscript. They also thank the beef cattle veterinarians, feedyard owners, managers, and staff for their initiation and continued facilitation of this work.

Conflict of interest

The author(s) declare that there is no conflict of interest.

Funding

This work was supported by the WD Farr Scholar: 32 HL007171 (GMK); the Integrated Livestock Management (FG); NIH/NHLBI Grants: P01 HL14985 and R01 HL114887; and a Department of Defense (DoD) Grant: PR140977 (KRS).

References

1. Centers for Disease Control and Prevention. *Prevalence of Obesity Among Adults and Youth: United States, 2011–2014*. Atlanta, GA: CDC, 2015.
2. Guazzi M. Pulmonary hypertension in heart failure preserved ejection fraction: prevalence, pathophysiology, and clinical perspectives. *Circ Heart Fail* 2014; 7: 367–377.
3. Cavalcante JL, Tamarappoo BK, Hachamovitch R, et al. Association of epicardial fat, hypertension, subclinical coronary artery disease, and metabolic syndrome with left ventricular diastolic dysfunction. *Am J Cardiol* 2012; 110: 1793–1798.
4. Robbins IM, Newman JH, Johnson RF, et al. Association of the metabolic syndrome with pulmonary venous hypertension. *Chest* 2009; 136: 31–36.
5. Haemers P, Hamdi H, Guedj K, et al. Atrial fibrillation is associated with the fibrotic remodelling of adipose tissue in the subepicardium of human and sheep atria. *Eur Heart J* 2017; 38: 53–61.

6. Bharati S and Lev M. Cardiac conduction system involvement in sudden death of obese young people. *Am Heart J* 1995; 129: 273–281.
7. Barnett CF and Selby VN. Overview of WHO Group 2 Pulmonary Hypertension Due to Left Heart Disease. *Advances in Pulmonary Hypertension* 2015; 14: 70–78.
8. Valero-Munoz M, Backman W and Sam F. Murine models of heart failure with preserved ejection fraction: a ''Fishing Expedition''. *JACC Basic Transl Sci* 2017; 2: 770–789.
9. Gyongyosi M, Pavo N, Lukovic D, et al. Porcine model of progressive cardiac hypertrophy and fibrosis with secondary postcapillary pulmonary hypertension. *J Transl Med* 2017; 15: 202.
10. Lee J, Xu Y, Lu L, et al. Multiple abnormalities of myocardial insulin signaling in a porcine model of diet-induced obesity. *Am J Physiol Heart Circ Physiol* 2010; 298: H310–319.
11. USDA-ERS. *Economic Research Service* 2017.
12. Owens FN, Gill DR, Secrist DS, et al. Review of some aspects of growth and development of feedlot cattle. *J Anim Sci* 1995; 73: 3152–3172.
13. Neary JM, Garry FB, Holt TN, et al. Mean pulmonary arterial pressures in Angus steers increase from cow-calf to feedlot-finishing phases. *J Anim Sci* 2015; 93: 3854–3861.
14. Neary JM, Booker CW, Wildman BK, et al. Right-sided congestive heart failure in North American feedlot cattle. *J Vet Intern Med* 2016; 30: 326–334.
15. Shirley KL, Beckman DW and Garrick DJ. Inheritance of pulmonary arterial pressure in Angus cattle and its correlation with growth. *J Anim Sci* 2008; 86: 815–819.
16. McLaughlin RF Jr, Tyler WS and Canada RO. A study of the subgross pulmonary anatomy in various mammals. *American Journal of Anatomy* 1961; 108: 149–165.
17. Alexander AF and Jensen R. Normal structure of bovine pulmonary vasculature. *Am J Vet Res* 1963; 24: 1083–1093.
18. Kay JM. Comparative morphologic features of the pulmonary vasculature in mammals. *Am Rev Respir Dis* 1983; 128: S53–57.
19. McLaughlin RF Jr. Bronchial artery distribution in various mammals and in humans. *Am Rev Respir Dis* 1983; 128: S57–58.
20. Ishibashi-Ueda H, Matsuyama TA, Ohta-Ogo K, et al. Significance and value of endomyocardial biopsy based on our own experience. *Circ J* 2017; 81: 417–426.
21. Dorfmuller P, Gunther S, Ghigna MR, et al. Microvascular disease in chronic thromboembolic pulmonary hypertension: a role for pulmonary veins and systemic vasculature. *Eur Respir J* 2014; 44: 1275–1288.
22. Gerges C, Gerges M, Lang MB, et al. Diastolic pulmonary vascular pressure gradient: a predictor of prognosis in ''out-of-proportion'' pulmonary hypertension. *Chest* 2013; 143: 758–766.
23. Assad TR, Hemnes AR, Larkin EK, et al. Clinical and biological insights into combined post- and pre-capillary pulmonary hypertension. *J Am Coll Cardiol* 2016; 68: 2525–2536.
24. Naeije R, Vachiery JL, Yerly P, et al. The transpulmonary pressure gradient for the diagnosis of pulmonary vascular disease. *Eur Respir J* 2013; 41: 217–223.
25. Simonneau G, Torbicki A, Dorfmuller P, et al. The pathophysiology of chronic thromboembolic pulmonary hypertension. *Eur Respir Rev* 2017; 26: 160112.
26. Andersen KH, Andersen CB, Gustafsson F, et al. Pulmonary venous remodeling in COPD-pulmonary hypertension and idiopathic pulmonary arterial hypertension. *Pulm Circ* 2017; 7: 514–521.
27. Fayyaz AU, Edwards WD, Maleszewski JJ, et al. Global pulmonary vascular remodeling in pulmonary hypertension associated with heart failure and preserved or reduced ejection fraction. *Circulation* 2018; 137: 1796–1810.
28. Hoeper MM, Lam CSP, Vachiery JL, et al. Pulmonary hypertension in heart failure with preserved ejection fraction: a plea for proper phenotyping and further research. *Eur Heart J* 2017; 38: 2869–2873.
29. Ghigna MR, Guignabert C, Montani D, et al. BMPR2 mutation status influences bronchial vascular changes in pulmonary arterial hypertension. *Eur Respir J* 2016; 48: 1668–1681.
30. Galambos C, Sims-Lucas S, Abman SH, et al. Intrapulmonary bronchopulmonary anastomoses and plexiform lesions in idiopathic pulmonary arterial hypertension. *Am J Respir Crit Care Med* 2016; 193: 574–576.
31. Alpert MA, Agrawal H, Aggarwal K, et al. Heart failure and obesity in adults: pathophysiology, clinical manifestations and management. *Curr Heart Fail Rep* 2014; 11: 156–165.
32. Iacobellis G and Bianco AC. Epicardial adipose tissue: emerging physiological, pathophysiological and clinical features. *Trends Endocrinol Metab* 2011; 22: 450–457.
33. Iacobellis G, Corradi D and Sharma AM. Epicardial adipose tissue: anatomic, biomolecular and clinical relationships with the heart. *Nat Clin Pract Cardiovasc Med* 2005; 2: 536–543.
34. Schafer K, Drosos I and Konstantinides S. Perivascular adipose tissue: epiphenomenon or local risk factor? *Int J Obes (Lond)* 2017; 41: 1311–1323.
35. Marchington JM, Mattacks CA and Pond CM. Adipose tissue in the mammalian heart and pericardium: structure, foetal development and biochemical properties. *Comp Biochem Physiol B* 1989; 94: 225–232.
36. Greenstein AS, Khavandi K, Withers SB, et al. Local inflammation and hypoxia abolish the protective anticontractile properties of perivascular fat in obese patients. *Circulation* 2009; 119: 1661–1670.
37. Cherian S, Lopaschuk GD and Carvalho E. Cellular cross-talk between epicardial adipose tissue and myocardium in relation to the pathogenesis of cardiovascular disease. *Am J Physiol Endocrinol Metab* 2012; 303: E937–949.
38. Drosos I, Chalikias G, Pavlaki M, et al. Differences between perivascular adipose tissue surrounding the heart and the internal mammary artery: possible role for the leptin-inflammation-fibrosis-hypoxia axis. *Clin Res Cardiol* 2016; 105: 887–900.
39. Hosogai N, Fukuhara A, Oshima K, et al. Adipose tissue hypoxia in obesity and its impact on adipocytokine dysregulation. *Diabetes* 2007; 56: 901–911.
40. Rausch ME, Weisberg S, Vardhana P, et al. Obesity in C57BL/6J mice is characterized by adipose tissue hypoxia and cytotoxic T-cell infiltration. *Int J Obes (Lond)* 2008; 32: 451–463.
41. Nosalski R and Guzik TJ. Perivascular adipose tissue inflammation in vascular disease. *Br J Pharmacol* 2017; 174: 3496–3513.
42. Venteclef N, Guglielmi V, Balse E, et al. Human epicardial adipose tissue induces fibrosis of the atrial myocardium through the secretion of adipo-fibrokines. *Eur Heart J* 2015; 36: 795–805a.

43. Cavalera M, Wang J and Frangogiannis NG. Obesity, metabolic dysfunction, and cardiac fibrosis: pathophysiological pathways, molecular mechanisms, and therapeutic opportunities. *Transl Res* 2014; 164: 323–335.
44. Iacobellis G, Ribaudo MC, Zappaterreno A, et al. Relation between epicardial adipose tissue and left ventricular mass. *Am J Cardiol* 2004; 94: 1084–1087.
45. Powell BD, Redfield MM, Bybee KA, et al. Association of obesity with left ventricular remodeling and diastolic dysfunction in patients without coronary artery disease. *Am J Cardiol* 2006; 98: 116–120.
46. Mahabadi AA, Massaro JM, Rosito GA, et al. Association of pericardial fat, intrathoracic fat, and visceral abdominal fat with cardiovascular disease burden: the Framingham Heart Study. *Eur Heart J* 2009; 30: 850–856.
47. *Veterinary Clinics: Food Animal Practice*. 2007.
48. McDonald P, Edwards RA, Greenhalgh JFD, et al. *Animal Nutrition*, 6th ed. Harlow, UK, 2002.
49. Drolet R, D'Allaire S and Chagnon M. Some observations on cardiac failure in sows. *Can Vet J* 1992; 33: 325–329.
50. Lee JC, Taylor FN and Downing SE. A comparison of ventricular weights and geometry in newborn, young, and adult mammals. *J Appl Physiol* 1975; 38: 147–150.
51. Wideman RF, Rhoads DD, Erf GF, et al. Pulmonary arterial hypertension (ascites syndrome) in broilers: a review. *Poult Sci* 2013; 92: 64–83.
52. Olkowski AA, Abbott JA and Classen HL. Pathogenesis of ascites in broilers raised at low altitude: aetiological considerations based on echocardiographic findings. *J Vet Med A Physiol Pathol Clin Med* 2005; 52: 166–171.
53. Olkowski AA, Rathgeber BM, Sawicki G, et al. Ultrastructural and molecular changes in the left and right ventricular myocardium associated with ascites syndrome in broiler chickens raised at low altitude. *J Vet Med A Physiol Pathol Clin Med* 2001; 48: 1–14.
54. Philbin E, Rocco T, Lindenmuth N, et al. Systolic versus diastolic heart failure in community practice: clinical features, outcomes, and the use of angiotensin-converting enzyme inhibitors. *Am J Med* 2000; 109: 605–613.